



Published in final edited form as:

Mol Pharm. 2016 February 01; 13(2): 420–427. doi:10.1021/acs.molpharmaceut.5b00653.

Metal Chelation Modulates Phototherapeutic Properties of Mitoxantrone-loaded Porphyrin–Phospholipid Liposomes

Kevin A. Carter, Sophie Wang, Jumin Geng, Dandan Luo, Shuai Shao, and Jonathan F. Lovell*

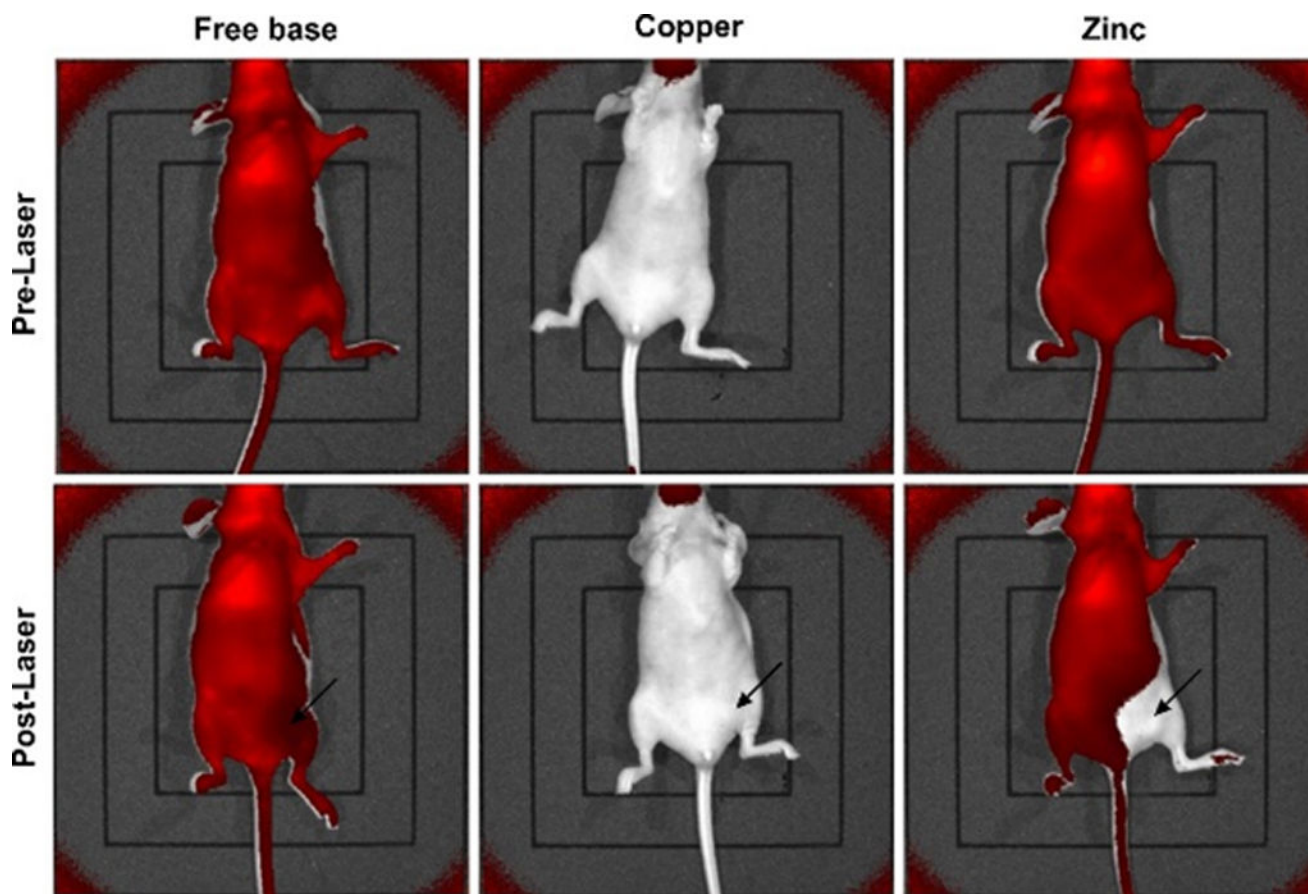
Department of Biomedical Engineering, University at Buffalo, State University of New York, Buffalo, NY, 14260

Abstract

Liposomes incorporating porphyrin–phospholipid (PoP) can be formulated to release entrapped contents in response to near infrared (NIR) laser irradiation. Here, we examine effects of chelating copper or zinc into the PoP. Cu(II) and Zn(II) PoP liposomes, containing 10 molar % HPPH-lipid, exhibited unique photophysical properties and released entrapped cargo in response to NIR light. Cu-PoP liposomes exhibited minimal fluorescence and reduced production of reactive oxygen species upon irradiation. Zn-PoP liposomes retained fluorescence and singlet oxygen generation properties, however they rapidly self-bleached under laser irradiation. Compared to the free base form, both Cu- and Zn-PoP liposomes exhibited reduced phototoxicity in mice. When loaded with mitoxantrone and administered intravenously at 5 mg/kg to mice bearing human pancreatic cancer xenografts, synergistic effects between the drug and the light treatment (for this particular dose and formulation) were realized with metallo-PoP liposomes. The drug-light-interval affected chemophototherapy efficacy and safety.

TOC Figure

*Correspondence: jflovell@buffalo.edu.



Keywords

Chemophototherapy; porphyrin-phospholipid; liposomes; mitoxantrone; metalloporphyrins; photobleaching; tumor ablation; light-triggered

Introduction

An ongoing goal of drug delivery systems is to deliver therapeutic payloads while reducing the total exposure of the drug to healthy tissues and organs. To this end, nanoparticles such as liposomes have shown promise as delivery vehicles and have achieved several examples of clinical translation.¹⁻⁴ This success can often be attributed to modulation of pharmacokinetics, reduction of injected excipients or reduction of negative side effects; as opposed to a straightforward improvement in therapeutic efficacy.⁵ Most nanocarriers depend on passive accumulation at the diseased site,^{5,6} which is less than ideal. For this reason, strategies where nanoparticles are preferentially targeted to the diseased site have been explored, such as the use of prodrugs, antibody targeting and external targeting.⁷⁻¹¹

As drug delivery vehicles, liposomes provide advantageous features such as biocompatibility, capacity for functionalization, reduction of side effects and ability to encapsulate high amounts of drugs.^{1,12} Remote loading through transmembrane gradients

enables the encapsulation of a variety of drugs at high concentrations including anti-cancer drugs such as doxorubicin (Dox) and mitoxantrone (MIT).¹³ Both drugs have been used clinically in polyethylene glycol-coated (PEGylated) liposomes, and a liposomal Dox formulation has achieved clinical approval.³ MIT has been evaluated in PEGylated liposomes in clinical trials.¹⁴ Liposomes provide a way of reducing the side effects associated with these drugs¹⁵, thereby improving their efficacy.^{12,16}

In theory, the use of external stimuli allows for precision treatment of a localized tumor and the potential to reduce the total injected drug dose. Such systems would involve the administration of a drug encapsulated in a nanoparticle which can be activated by an external stimulus such as heat, light magnetic fields or ultrasound.¹⁷ While many types of drug-loaded nanoparticles have been developed to respond to an external stimulus thus far only one, a heat triggered doxorubicin liposomal formulation, has been tested in advanced clinical trials.^{18,19} We have previously shown that liposomes made with porphyrin–phospholipid (PoP) are capable of releasing cargo under laser irradiation, and drug release in the tumor may provide advantages over other triggering mechanisms.^{20–22} Porphyrins have a long history of use in theranostic applications and are also being used for new approaches to photomedicine.^{23,24}

In a previous study²⁰ 2-[1-hexyloxyethyl]-2-devinyl pyropheophorbide-*a* (HPPH)-lipid was added to a liposomal formulation consisting of distearoylphosphatidylcholine (DSPC), 1,2-distearoyl-sn-glycero-3-phosphoethanolamine-N-(methoxy(PEG)-2000) (DSPE-PEG2K), and cholesterol (molar ratio 60:5:35). It was shown that replacing 10% (molar) DSPC with 10% (molar) HPPH-lipid allowed the liposomes to release their contents when treated with a near infrared (NIR) laser. This liposomal formulation, when loaded with Dox was shown to be effective at ablating KB tumor xenografts with a single NIR chemophototherapy treatment. However, the liposome composition contained a relatively high amount of HPPH-lipid, meaning the dose limiting factors could be the amount of photosensitizer applied. High photosensitizer doses can lead to two problems; phototoxicity under laser irradiation²⁵ and prolonged skin sunlight phototoxicity if the photosensitizer is not rapidly cleared.^{25–28} Skin toxicity might be increased in the case of PoP liposomes as the enhanced circulation time of PEGylated liposomes increases the accumulation of liposomes in the skin.^{29,30}

One way to reduce phototoxic effects of the porphyrins is to chelate a metal such as Cu^{31,32} which has been shown to quench singlet oxygen production. Metals have been shown to change functional and spectral properties of photosensitizers and add novel functionality.^{33–39} These include altering the cellular uptake, adding contrast agent functionality, or altering the photoactivity and efficacy.^{40–42}

Metallo-PoP liposomes in particular have been demonstrated to have unique properties and functions. When chelated with cobalt, PoP liposomes enable the binding of his-tag labeled proteins,⁴³ While the addition of ⁶⁴Cu and Mn allow the liposomes and other tetrapyrrolic nanoparticles to be readily used as PET and magnetic resonance imaging contrast agents.^{44–47} To the best of our knowledge, metallo-PoP liposomes have not been evaluated for therapeutic activity.

Here, we demonstrate the effects of Cu and Zn chelation on the phototherapeutic properties of drug-loaded PoP liposomes. The use of metalloporphyrins in PoP liposomes is shown to change the spectral and functional characteristics of the liposomes. The addition of transition metals alters the photoreactive species generating capacities of the liposomes along with their cargo loading and release characteristics, and behavior under NIR laser irradiation. The changes in these characteristics allow for in-vivo applications which would not be possible using equal dosing of the free base form of the PoP. Liposomes comprising 10 molar % free base HPPH-lipid Cu-HPPH-lipid and Zn-HPPH-lipid were evaluated for their photodynamic effects on tumor growth, and the therapeutic effects of using them to deliver antineoplastic drugs to tumors. It has been shown previously that a PDT treatment in conjunction with drug and nanoparticles enhances the tumor drug accumulation and provides a synergistic tumor growth inhibition effect.⁴⁸⁻⁵³

Depending on the precise formulation, PoP liposomes function through combined effects of PDT, drug accumulation following light treatment and the release of the drug from the liposomes following tumor accumulation. With this in mind, we have developed metallo-HPPH-lipids which have the potential of reducing phototoxicity while retaining the therapeutic effects of PoP liposomes.

Experimental

HPPH-lipid synthesis and liposome preparation:

HPPH-lipid was synthesized as previously described²⁰ and metal chelation was accomplished as recently described, but using HPPH-lipid in place of pyro-lipid.⁴³ Cu-PoP was synthesized by combining free base HPPH PoP with 10 excess folds of anhydrous copper(II) acetate dissolved in 4 mL tetrahydrofuran. The mixture was left in dark for 3 hours with stirring. Similarly Zn-PoP was synthesized in the same manner with 10 excess folds of zinc(II) acetate dihydrate in 4 mL methanol. The mixture was left in dark overnight with stirring. Reaction progress could be monitored by sampling small volumes and subjecting these to silica gel thin layer chromatography with a mobile phase with a volume ratio of [chloroform:methanol:water]; [65:25:4]. The solvent was removed by rotary evaporation and the residue was extracted by chloroform/methanol/water 1:1.8:1 (volume ratio) three times. The chloroform layer was collected, the solvent was removed by rotary evaporation and the product was freeze-dried to give a fine powder.

Liposome were prepared either by the film hydration method (smaller scale) or by the hot ethanol injection method (larger scales). Lipid films were prepared by drying chloroform solutions containing DSPC (Avanti, # 850365P), DSPE-PEG2K (Avanti, # 880120P), HPPH-lipid (free base or metal chelated derivatives) and cholesterol (Avanti, # 700000P) in the molar ratios of 50:5:10:35 (DSPC:DSPE:DSPE-PEG2K:HPPH-lipid:Chol) under an argon stream. The films were kept overnight under vacuum to remove residual chloroform. To prepare liposomes, the films were re-hydrated with phosphate-buffered saline (pH 7.4), producing a solution with a final lipid concentration of 10 mg/mL, and sonicated for 30 minutes at 60 °C. Liposomes loaded with drugs were prepared by dissolving lipids at the indicated molar ratios in ethanol at 60 °C and adding ammonium sulfate for a final solution that is 20% ethanol v/v and a lipid concentration of 20 mg/mL. The solution was then

extruded 10 times through stacked 80, 100, 200 nm polycarbonate membranes. Following extrusion the liposomes were dialyzed overnight in a 10% sucrose buffer with 10 mM HEPES pH 7.4. The dialyzed liposomes were loaded with drugs at a lipid to drug molar ratio of 10:1 at 60 °C for 30 minutes to 1 hour. Loading efficacy was determined by separating untrapped free drug from liposomes using a Sephadex G-75 (GE Health) column (inclusion range up to 80 kDa), collecting 24, 1 mL fractions. Loading efficiency was calculated by comparing the drug fluorescence intensity of non-liposome fractions for a given sample pre- and post-incubation. Drug fluorescence intensity was calculated by the area under the curve. Size and polydispersity were measured by dynamic light scattering in a NanoBrook 90 plus PALS in PBS. Zeta potential was measured in a 1 mM NaCl solution.

Spectral Experiments:

Emission spectra were recorded for the three types of HPPH-lipid (Cu, Zn and freebase) in methanol. Equal concentrations of each lipid were dissolved in methanol and the emission spectra were recorded with an excitation of 400 nm using a PTI fluorimeter. For bleaching experiments, fluorescence measurements were taken before and after treatment with laser for intact and lysed (with 2.5% Triton-X100) liposomes. The laser treatment was conducted with a 665 nm laser at a fluence rate of 200 mW/cm² for 60 seconds in a 3 mL cuvette with stirring. Fluorescence measurements were done in a PTI fluorimeter with an excitation of 400 nm. Bleaching of the porphyrin was calculated by comparing the fluorescence of the HPPH-lipids at 665 nm post laser to the pre laser values of lysed liposomes. All liposomes were lysed to compare the total bleaching to an untreated sample, to avoid any effects which may be induced by self-quenching. Absorbance measurements of liposomes were recorded for liposomes which were laser treated identically to the fluorescence bleaching experiments. For consistency, all liposomes were lysed with 0.25% Triton X-100 before absorbance measurements were made.

Singlet Oxygen Generation:

Singlet oxygen sensor green (SOSG, Molecular Probes, # S36002) was used to study the generation of singlet oxygen. Liposomes (5 nM PoP) were added to a 0.5 μM SOSG solution and irradiated at 200 mW/cm² for 15 second. The fluorescence of SOSG was measured using excitation/emission of 504/525 nm before and after laser treatment. The fold increase was calculated by dividing the post-laser value by the pre-laser value.

Drug Release and Stability:

Due to overlapping fluorescence wavelengths between HPPH and MIT, it was not possible to read the fluorescence of the MIT in the presence of HPPH. As a result, it was necessary to use a method for determining loading efficiency and laser triggered release. The most efficient way to do this was to run the laser treated liposomes over a Sephadex G-75 column. As we have previously shown the laser treatment permeabilizes the liposomes without destroying their structure²⁰, it was possible to use G-75 columns to separate the liposomes from any free drug released during laser treatment. Liposomes were diluted in PBS and treated with a 665 nm laser for 10 minutes at a fluence rate of 200 mW/cm². The treated liposomes were then run through a G-75 column to separate the free (released) drug from the drug still entrapped in the liposomes. Release was calculated by comparing the MIT

fluorescence in non-liposome fractions to the fluorescence of an equal concentration of free MIT. Dox release was calculated by comparing the fluorescence before and after laser treatment and disruption with Triton X-100 using the equation $(F_{\text{fin}}-F_{\text{int}})/(F_{\text{x100}}-F_{\text{int}})\times 100\%$. Dox fluorescence was read with excitation/emission of 480/590 nm and MIT fluorescence at 607/688 nm in a Tecan plate reader. Serum stability was measured similarly to light release. Liposomes were incubated in 50% adult bovine serum at 37 °C (Pel-Freez #37218-5) for 24 hours and drug release was assessed using fluorescence.

Survival experiments:

Animal experiments were carried out in accordance to protocols approved by the University at Buffalo Institutional Animal Care and Use Committee. 4–5 week old female nude mice (Jackson Labs) were inoculated with 5×10^6 MIA PaCa-2 human pancreatic cancer derived cells on the left groin. When tumors reached 4–6 mm in diameter mice were placed in one of 13 groups (n=5–7). MIT-loaded PoP liposomes (5mg/kg MIT) or an equivalent dose of empty PoP liposomes were injected via tail-vein. Injected mice were treated 10 minutes or 24 hours following injections for 12.5 minutes with a 665 nm laser at a fluence rate of 200 mW/cm² laser (total fluence of 150 J/cm²). Tumor size was measured 3 times a week and mice were sacrificed if the tumor grew larger than 5 times the initial volume or after 90 days.

In vivo imaging experiments:

For imaging experiments, nude mice bearing MIA-PaCa-2 tumors were injected with HPPH liposomes at a dose of 11 mg/kg HPPH-lipid (the equivalent of 5 mg/kg MIT). 24 hours following injections, (when the HPPH-lipid is partially unquenched and liposomes have extravasated into the skin) the mice were treated on the indicated locations and imaged before and after laser treatment with an IVIS imaging system (Excitation: 665 nm filter, Emission: Cy 5.5 filter). These results were confirmed with CD-1 mice (4 week females, Harlan Laboratories). Fur on the right flank on the mice was removed using clippers and hair removal cream. The mice were injected and treated as the nude mice. Similar results were observed in all treated mice (n=3). The fluorescence bleaching was quantified by analyzing the treated spots using region of interest (ROI) analysis in the IVIS software.

Statistical analysis:

Kaplan-Meier survival curves were analyzed using Graphpad prism (Version 5.01) software. Each pair of groups were compared by Log-rank (Mantel-Cox) test. Differences were considered significant at $p < 0.05$. Median survival is defined as the time at which the staircase survival curve crosses the 50% survival point.

Results and Discussion

Liposome photophysical properties

Cu and Zn PoP were based on HPPH-phospholipid (synthesized as recently described²⁰), chelated with metals (carried out as recently described⁴³) at the center of the porphyrin (Fig 1A). These metallo-PoPs had greater than >90% purity based on HPLC (Fig S1 in the Supporting Information). They were incorporated into liposomes containing DSPC:DSPE:DSPE-PEG2K:PoP:Cholesterol (molar ratio 50:5:10:35) and could be

successfully formed using either hot ethanol injection and extrusion, or sonication. The chelation of metals into porphyrins is known to alter fluorescence and other properties.⁵⁴ Cu, for example can attenuate the fluorescence,⁵⁵ which itself can be used as a proxy for the singlet oxygen generation capacity of the porphyrin.⁵⁶ Both Cu and Zn PoP liposomes exhibited reduced fluorescence compared to the metal free base PoP liposomes (Fig. 1B). Cu-PoP liposomes showed more than a 95% reduction in fluorescence, while Zn-PoP liposomes showed only a slight decrease, which might be attributed to the rapid self-bleaching of the Zn porphyrin under ambient light.

Under laser irradiation, porphyrins eventually self-bleach due to reactions with the generated singlet oxygen⁵⁷, a process which to completely bleach the porphyrin typically requires the application of large light doses. Zn-PoP liposomes had a very high rate of self-bleaching, compared to the free base and Cu-PoP (Fig. 1C). When the three types of PoP liposomes derivatives were treated with a 665 nm laser for 60 seconds at 200 mW/cm², the free base and Cu showed no significant bleaching in the lysed form and limited bleaching for intact liposomes. In contrast, the Zn had an almost complete reduction of its fluorescence. This self-bleaching was found to be more pronounced when the liposomes were lysed than when in the intact liposomal form. To study the effects of Cu (low fluorescence) and Zn (high self-bleaching) on HPPH-lipid singlet oxygen generation, the molecular probe singlet oxygen sensor green (SOSG) was used. As shown in Fig 1D, the free base in its lysed form generated significantly more singlet oxygen than any of the other samples. Cu did not induce a large increase in SOSG activity, however the intact sample showed a greater increase than the lysed sample. Zn induced little increase in SOSG signal when intact and significantly more when lysed, as would be expected from the bleaching result. The self-bleaching of the Zn-PoP was accompanied by a reduction in the absorbance (Fig 2), which did not occur in the free base or Cu PoP liposomes treated under the same conditions. However, when treated for longer times the absorbance of both the free base and Cu also decreased, although they required significantly more time for results similar to that of the Zn. The mechanism of the photobleaching is unclear, but oxidative photobleaching is a well-known phenomenon observed for photosensitizers.⁵⁸

In-vivo imaging

Nude mice were injected intravenously with equal doses of free base, Cu and Zn PoP liposomes (11 mg/kg HPPH-lipid), and treated with a 665 nm laser for 12.5 minutes at 200 mW/cm² (150 J/cm²) 24 hours following injection, when the HPPH is unquenched. Mice were imaged before and after laser treatment. The laser treatment induced limited bleaching in the mice injected with the free base and complete bleaching at the treated location in the mice injected with Zn (Fig 3). Cu-PoP liposome treated mice did not show any significant fluorescence in either pre or post laser images. ROI analysis of similarly treated CD-1 mice showed a 3 fold decrease in fluorescence of the free base group, a 7 fold decrease for the Zn group, and no significant difference between in Cu group (Fig S2 in the Supporting Information).

Drug loading and stability

It has previously been shown that liposomes containing PoP can actively load drugs such as doxorubicin when the formulation contains a type of PoP which can form a stable bilayer with the appropriate phospholipid composition.^{20,59} Doxorubicin can be stably loaded into liposomes consisting of 10% (molar) free base HPPH-lipid.²⁰ Metalloporphyrins were able to form liposomes with similar characteristics as the free base PoP (Fig S3 in the Supporting Information). However, Dox proved difficult to stably load consistently into metal-PoP liposomes. For this reason we explored the use of another drug, mitoxantrone (MIT), an anthraquinone which can be actively loaded into liposomes.^{16,60} Liposomes loaded with MIT showed high (>90%) loading efficiencies while liposomes loaded with Dox showed lower and inconsistent loading (Fig 4A). The effect of the metals on the stability of the liposomes was studied assessed in 50% serum at 37 °C. MIT loaded liposomes had the greatest stability with less than 10% release for free base and less than 25% for Cu and Zn PoP after 24 hours. Free base Dox-loaded PoP liposomes were stable however both Cu and Zn Dox-loaded PoP liposomes were not, with more than 90% drug release (Fig 4B). The effects of the metals on light triggered release was tested for both Dox and MIT liposomes treated for 10 minutes at 200 mW/cm² (Fig 4C). Both free base and Zn showed more than 85% release following light treatment. In the case of Cu, very little release was observed immediately after light treatment. However, over time Dox was slowly released up to two hours following light treatment (Fig 4D).

In vivo efficacy

MIT-loaded PoP liposomes were used for in-vivo experiments. Mice were injected with 5 mg/kg MIT PoP liposomes and treated either 10 minutes or 24 hours following IV injection at a fluence rate of 200 mW/cm² for 12.5 minutes (150 J/cm²). Mice treated at a 10 minute drug-light-interval following injection showed delay in tumor growth for both empty and loaded liposomes compared to saline (median survival = 12 days) (Fig 5). The groups treated with free base PoP showed no significant differences between the loaded and empty liposome treatments (median survival = 38 days for both). Cu-PoP loaded and empty (21 vs 19 days) and Zn-PoP loaded and empty (35 vs 21 days) liposome groups showed statistically significant differences between the treatments with or without MIT ($P < 0.05$).

The mice that were treated at a 24 hour drug-light-interval also exhibited delayed tumor growth, with the striking exception of mice treated with the free base PoP, which had to be sacrificed due to severe phototoxicity induced by the light treatment (Fig 6). The Cu-PoP (MIT-loaded and empty; 19 and 17 days median survival respectively) groups showed a significant ($P < 0.05$). survival improvement compared to the saline group, as did the Zn-PoP (MIT-loaded and empty; 43 and 38 days median survival). However, there was no significant difference in survival with phototreatments using the MIT-loaded and empty metallo-PoP liposomes at the 24 hour drug-light-interval. The lack of differences between the loaded and empty liposome can be attributed to either lower circulating drug concentrations, a stronger PDT effect at 24 hours due to tumor uptake and unquenching, or a combination of both. Of all the groups, those treated with Zn-PoP at 24 hours showed the greatest increase in survival time, followed closely by free base treated at 10 minutes. Groups treated with Cu-PoP showed similar results for treatments done at 10 minutes and 24 hours, suggesting the

efficacy is due to a mild PDT effect rather than a drug-induced effect. Similarly, the treatment of Zn-PoP at 24 hours shows that a PDT effect is the dominant factor contributing to its efficacy, whereas the treatments done at 10 minutes which showed a significant difference between the MIT-loaded and empty groups suggests that at the right dose of drug-loaded liposomes can have greater efficacy as has been shown previously.^{20,21}

Metallo-PoP liposomes demonstrated unique properties which may make their use advantageous compared to the free base form in certain circumstances. The inclusion of either Cu or Zn improved the safety of the liposomes while maintaining the liposomes ability to function as a therapeutic and drug delivery agent. While the addition of the metals reduced the therapeutic efficacy compared to the freebase at a MIT dose of 5 mg/kg, higher doses may have allowed the Zn-PoP to be equally as effective, as demonstrated in pilot studies using 10 mg/kg (Fig S4 in the Supporting Information). Cu-PoP significantly reduced the singlet oxygen generating capacity of the liposomes, rendering them safer than the other variations tested. With limited singlet oxygen generation, Cu-PoP liposomes did not provide sufficient therapeutic effectiveness in the formulations tested, since these likely relied on a photodynamic effect to permeabilize tumor vasculature and enhance liposome accumulation, a phenomena known to occur when PDT treatment is used with nanoparticles^{48,53} and plays a key role in the efficacy of PoP liposomes. Zn-PoP liposomes retained the capacity to induce permeabilization of tumor vasculature and could be effective at enhancing the delivery of drugs to the target site, while minimizing the potential for phototoxic reactions. The free base form was safe when used immediately following injection but not 24 hours post injection. This can be attributed to the fact that the HPPH is quenched when the liposomes are intact (as they are during the early time points following injection), as is the singlet oxygen generation of the HPPH-lipid⁵⁶. Over time, the HPPH fluorescence is unquenched in the blood and in organs where the liposomes have accumulated as they are broken down. The use of Zn-HPPH-lipid solves this problem as it rapidly self-bleaches under laser irradiation when the liposomes are unquenched thereby reducing potential for phototoxicity. This was clearly demonstrated in the groups treated at 24 hours. The free base showed significant toxicity which made the treatment fatal whereas the Zn-PoP groups showed no signs of phototoxicity and improved tumor growth suppression compared to the Zn-PoP groups treated at 10 minutes post injection.

Unlike our previously published results showing a strong synergistic effect between the drug and phototreatment for Dox-loaded free base PoP liposomes^{20,21}, MIT PoP liposomes with this particular formulation behaved differently. While the benefits of the drug loaded liposomes shown here were relatively modest, they could be seen in the Zn-PoP liposome groups treated at 10 minutes. Higher drug doses may help to provide greater survival in groups treated with the drug while not significantly increasing the effect of the empty liposomes. The combination of the high photosensitizer and light doses used in this treatment would likely lead to oxygen depletion⁶¹. Increasing the drug dose may improve the tumor drug accumulation and consequently its efficacy.

Metallo-PoP liposomes demonstrated unique properties which may have applications in reducing the toxicities associated with the use of the free base porphyrins. Zn HPPH-lipid provided a reduction in phototoxicity through its rapid self-bleaching properties while

maintaining an anti-tumor effect. While Cu HPPH-lipid demonstrated the ability to reduce singlet oxygen generation, it also showed less favorable therapeutic efficacy, demonstrating that for this treatment with this particular formulation, a photodynamic effect was beneficial. However, Cu-PoP might be appropriate to induce release of cargo in extravasated liposomes to improve drug efficacy without photodynamic effect, although the suitability of Cu-PoP for this such an application requires further study at higher drug doses. Both metal forms of HPPH-lipid demonstrated the ability to provide a therapeutic benefit and with modifications and additional development could be used to deliver anti-tumor drugs in light-triggered liposomes with diminished phototoxicity associated with the use of photosensitizers.

Conclusion

The use of metallo-PoP liposomes imparts unique properties which have been demonstrated to affect to safety of the liposomes when used as a delivery system for anti-cancer drugs. The improved safety may allow for future applications in which the use of large amounts of the free base form of the PoP would not be feasible due to risks of phototoxicity. Cu-PoP liposomes hold potential to be used for drug delivery based on mechanisms solely related to triggered release. Zn-PoP liposomes might be used for drug delivery based both on tumor vascular damage, drug-releasing mechanisms, together with photosensitization with a self-limiting capacity for phototoxicity.

Supplementary Material

Refer to Web version on PubMed Central for supplementary material.

Acknowledgements

This work was supported by grants from the National Institutes of Health (R01EB017270 and R21EB019147).

References

- (1). Allen TM; Cullis PR Liposomal Drug Delivery Systems: From Concept to Clinical Applications. *Adv. Drug Deliv. Rev* 2013, 65 (1), 36–48. [PubMed: 23036225]
- (2). Immordino ML; Dosio F; Cattel L Stealth Liposomes: Review of the Basic Science, Rationale, and Clinical Applications, Existing and Potential. *Int. J. Nanomedicine* 2006, 1 (3), 297–315. [PubMed: 17717971]
- (3). Barenholz Y Doxil® — The First FDA-Approved Nano-Drug: Lessons Learned. *J. Controlled Release* 2012, 160 (2), 117–134.
- (4). Kingsley JD; Dou H; Morehead J; Rabinow B; Gendelman HE; Destache CJ Nanotechnology: A Focus on Nanoparticles as a Drug Delivery System. *J. Neuroimmune Pharmacol* 2006, 1 (3), 340–350. [PubMed: 18040810]
- (5). Allen TM; Cullis PR Drug Delivery Systems: Entering the Mainstream. *Science* 2004, 303 (5665), 1818–1822. [PubMed: 15031496]
- (6). Maruyama K Intracellular Targeting Delivery of Liposomal Drugs to Solid Tumors Based on EPR Effects. *Adv. Drug Deliv. Rev* 2011, 63 (3), 161–169. [PubMed: 20869415]
- (7). Mills JK; Needham D Targeted Drug Delivery. *Expert Opin. Ther. Pat* 1999, 9 (11), 1499–1513.
- (8). Koo OM; Rubinstein I; Onyukel H Role of Nanotechnology in Targeted Drug Delivery and Imaging: A Concise Review. *Nanomedicine Nanotechnol. Biol. Med* 2005, 1 (3), 193–212.
- (9). Freeman AI; Mayhew E Targeted Drug Delivery. *Cancer* 1986, 58 (S2), 573–583. [PubMed: 3521839]

- (10). Ganta S; Devalapally H; Shahiwala A; Amiji M A Review of Stimuli-Responsive Nanocarriers for Drug and Gene Delivery. *J. Controlled Release* 2008, 126 (3), 187–204.
- (11). Luo D; Carter KA; Lovell JF *Nanomedical Engineering: Shaping Future Nanomedicines*. Wiley Interdiscip. Rev. Nanomed. Nanobiotechnol 2015, 7 (2), 169–188. [PubMed: 25377691]
- (12). Allen TM; Martin FJ *Advantages of Liposomal Delivery Systems for Anthracyclines*. *Semin. Oncol* 2004, 31 (6 Suppl 13), 5–15. [PubMed: 15717735]
- (13). Cern A; Golbraikh A; Sedykh A; Tropsha A; Barenholz Y; Goldblum A *Quantitative Structure - Property Relationship Modeling of Remote Liposome Loading of Drugs*. *J. Controlled Release* 2012, 160 (2), 147–157.
- (14). Yang J; Shi Y; Li C; Gui L; Zhao X; Liu P; Han X; Song Y; Li N; Du P; Zhang S *Phase I Clinical Trial of Pegylated Liposomal Mitoxantrone plm60-S: Pharmacokinetics, Toxicity and Preliminary Efficacy*. *Cancer Chemother. Pharmacol* 2014, 74 (3), 637–646. [PubMed: 25034977]
- (15). Safra T; Muggia F; Jeffers S; Tsao-Wei DD; Groshen S; Lyass O; Henderson R; Berry G; Gabizon A *Pegylated Liposomal Doxorubicin (doxil): Reduced Clinical Cardiotoxicity in Patients Reaching or Exceeding Cumulative Doses of 500 mg/m²*. *Ann. Oncol* 2000, 11 (8), 1029–1033. [PubMed: 11038041]
- (16). Li C; Cui J; Wang C; Li Y; Zhang H; Wang J; Li Y; Zhang L; Zhang L; Guo W; Wang Y *Encapsulation of Mitoxantrone into Pegylated SUVs Enhances Its Antineoplastic Efficacy*. *Eur. J. Pharm. Biopharm* 2008, 70 (2), 657–665. [PubMed: 18582570]
- (17). Caldorera-Moore M; Guimard N; Shi L; Roy K *Designer Nanoparticles: Incorporating Size, Shape, and Triggered Release into Nanoscale Drug Carriers*. *Expert Opin. Drug Deliv* 2010, 7 (4), 479–495. [PubMed: 20331355]
- (18). Needham D; Anyarambhatla G; Kong G; Dewhirst MW *A New Temperature-Sensitive Liposome for Use with Mild Hyperthermia: Characterization and Testing in a Human Tumor Xenograft Model*. *Cancer Res* 2000, 60 (5), 1197–1201. [PubMed: 10728674]
- (19). Poon RTP; Borys N *Lyso-Thermosensitive Liposomal Doxorubicin: A Novel Approach to Enhance Efficacy of Thermal Ablation of Liver Cancer*. *Expert Opin. Pharmacother* 2009, 10 (2), 333–343. [PubMed: 19236203]
- (20). Carter KA; Shao S; Hoopes MI; Luo D; Ahsan B; Grigoryants VM; Song W; Huang H; Zhang G; Pandey RK; Geng J; Pfeifer BA; Scholes CP; Ortega J; Karttunen M; Lovell JF *Porphyrim-phospholipid Liposomes Permeabilized by near-Infrared Light*. *Nat. Commun* 2014, 5.
- (21). Luo D; Carter KA; Razi A; Geng J; Shao S; Giraldo D; Sunar U; Ortega J; Lovell JF *Doxorubicin Encapsulated in Stealth Liposomes Conferred with Light-Triggered Drug Release*. *Biomaterials* 2016, 75, 193–202. [PubMed: 26513413]
- (22). Luo D; Carter KA; Razi A; Geng J; Shao S; Lin C; Ortega J; Lovell JF *Porphyrim-Phospholipid Liposomes with Tunable Leakiness*. *J. Controlled Release* 2015, 220, Part A, 484–494.
- (23). Zhang Y; Lovell JF *Porphyrim as Theranostic Agents from Prehistoric to Modern Times*. *Theranostics* 2012, 2 (9), 905–915. [PubMed: 23082102]
- (24). Huang H; Song W; Rieffel J; Lovell JF *Emerging Applications of Porphyrim in Photomedicine*. *Front Phys* 2015, 3, 23. [PubMed: 28553633]
- (25). Ferrario A; Gomer CJ *Systemic Toxicity in Mice Induced by Localized Porphyrim Photodynamic Therapy*. *Cancer Res* 1990, 50 (3), 539–543. [PubMed: 2137023]
- (26). Wooten RS; Smith KC; Ahlquist DA; Muller SA; Balm RK *Prospective Study of Cutaneous Phototoxicity after Systemic Hematoporphyrin Derivative*. *Lasers Surg. Med* 1988, 8 (3), 294–300. [PubMed: 2969070]
- (27). Veenhuizen RB; Ruevekamp-Helmers MC; Helmerhorst TJM; Kenemans P; Mooi WJ; Marijnissen JPA; Stewart FA *Intraperitoneal Photodynamic Therapy in the Rat: Comparison of Toxicity Profiles for Photofrin and mTHPC*. *Int. J. Cancer* 1994, 59 (6), 830–836. [PubMed: 7989125]
- (28). Wolford ST; Novicki DL; Kelly B *Comparative Skin Phototoxicity in Mice with Two Photosensitizing Drugs: Benzoporphyrin Derivative Monoacid Ring A and Porfimer Sodium (Photofrin)*. *Toxicol. Sci* 1995, 24 (1), 52–56.

- (29). Lotem M; Hubert A; Lyass O; Goldenhersh MA; Ingber A; Peretz T; Gabizon A Skin Toxic Effects of Polyethylene Glycol-Coated Liposomal Doxorubicin. *Arch. Dermatol* 2000, 136 (12), 1475–1480. [PubMed: 11115157]
- (30). Charrois GJR; Allen TM Rate of Biodistribution of STEALTH® Liposomes to Tumor and Skin: Influence of Liposome Diameter and Implications for Toxicity and Therapeutic Activity. *Biochim. Biophys. Acta BBA - Biomembr* 2003, 1609 (1), 102–108.
- (31). Carlsson DJ; Suprunchuk T; Wiles DM The Quenching of Singlet Oxygen (1 g) by Transition Metal Chelates. *Can. J. Chem* 1974, 52 (22), 3728–3737.
- (32). Joshi PC Copper(II) as an Efficient Scavenger of Singlet Molecular Oxygen. *Indian J. Biochem. Biophys* 1998, 35 (4), 208–215. [PubMed: 9854900]
- (33). Josefsen LB; Boyle RW Photodynamic Therapy and the Development of Metal-Based Photosensitisers. *Met.-Based Drugs* 2008, 2008.
- (34). Fan J; Whiteford JA; Olenyuk B; Levin MD; Stang PJ; Fleischer EB Self-Assembly of Porphyrin Arrays via Coordination to Transition Metal Bisphosphine Complexes and the Unique Spectral Properties of the Product Metallacyclic Ensembles. *J. Am. Chem. Soc* 1999, 121 (12), 2741–2752.
- (35). Sweigert P; Xu Z; Hong Y; Swavey S Nickel, Copper, and Zinc Centered Ruthenium-Substituted Porphyrins: Effect of Transition Metals on Photoinduced DNA Cleavage and Photoinduced Melanoma Cell Toxicity. *Dalton Trans* 2012, 41 (17), 5201–5208. [PubMed: 22414966]
- (36). Sessler JL; Tomat E Transition-Metal Complexes of Expanded Porphyrins. *Acc. Chem. Res* 2007, 40 (5), 371–379. [PubMed: 17397134]
- (37). Humphrey JL; Kuciauskas D Charge Transfer Enhances Two-Photon Absorption in Transition Metal Porphyrins. *J. Am. Chem. Soc* 2006, 128 (12), 3902–3903. [PubMed: 16551085]
- (38). Hannah S; Lynch V; Guldi DM; Gerasimchuk N; MacDonald CLB; Magda D; Sessler JL Late First-Row Transition-Metal Complexes of Texaphyrin. *J. Am. Chem. Soc* 2002, 124 (28), 8416–8427. [PubMed: 12105923]
- (39). Mitra S; Foster TH Photochemical Oxygen Consumption Sensitized by a Porphyrin Phosphorescent Probe in Two Model Systems. *Biophys. J* 2000, 78 (5), 2597–2605. [PubMed: 10777756]
- (40). Chen CW; Cohen JS; Myers CE; Sohn M Paramagnetic Metalloporphyrins as Potential Contrast Agents in NMR Imaging. *FEBS Lett* 1984, 168 (1), 70–74. [PubMed: 6705923]
- (41). Pavani C; Uchoa AF; Oliveira CS; Yamamoto Y; Baptista MS Effect of Zinc Insertion and Hydrophobicity on the Membrane Interactions and PDT Activity of Porphyrin Photosensitizers. *Photochem. Photobiol. Sci* 2009, 8 (2), 233–240. [PubMed: 19247516]
- (42). Garbo GM; Fingar VH; Wieman TJ; Iii EBN; Haydon PS; Cerrito PB; Kessel DH; Morgan AR In Vivo and In Vitro Photodynamic Studies with Benzochlorin Iminium Salts Delivered by a Lipid Emulsion. *Photochem. Photobiol* 1998, 68 (4), 561–568. [PubMed: 9796439]
- (43). Shao S; Geng J; Ah Yi H; Gogia S; Neelamegham S; Jacobs A; Lovell JF Functionalization of Cobalt Porphyrin–phospholipid Bilayers with His-Tagged Ligands and Antigens. *Nat. Chem* 2015, 7 (5), 438–446. [PubMed: 25901823]
- (44). Liu TW; MacDonald TD; Shi J; Wilson BC; Zheng G Intrinsically Copper-64-Labeled Organic Nanoparticles as Radiotracers. *Angew. Chem. Int. Ed Engl* 2012, 51 (52), 13128–13131. [PubMed: 23154923]
- (45). MacDonald TD; Liu TW; Zheng G An MRI-Sensitive, Non-Photobleachable Porphysome Photothermal Agent. *Angew. Chem. Int. Ed Engl* 2014, 53 (27), 6956–6959. [PubMed: 24840234]
- (46). Rieffel J; Chen F; Kim J; Chen G; Shao W; Shao S; Chitgupi U; Hernandez R; Graves SA; Nickles RJ; Prasad PN; Kim C; Cai W; Lovell JF Hexamodal Imaging with Porphyrin-Phospholipid-Coated Upconversion Nanoparticles. *Adv. Mater* 2015, 27 (10), 1785–1790. [PubMed: 25640213]
- (47). Zhang Y; Jeon M; Rich LJ; Hong H; Geng J; Zhang Y; Shi S; Barnhart TE; Alexandridis P; Huiyinga JD; Seshadri M; Cai W; Kim C; Lovell JF Non-Invasive Multimodal Functional Imaging of the Intestine with Frozen Micellar Naphthalocyanines. *Nat. Nanotechnol* 2014, 9 (8), 631–638. [PubMed: 24997526]

- (48). Snyder JW; Greco WR; Bellnier DA; Vaughan L; Henderson BW Photodynamic Therapy: A Means to Enhanced Drug Delivery to Tumors. *Cancer Res* 2003, 63 (23), 8126–8131. [PubMed: 14678965]
- (49). He P; Ahn J-C; Shin J-I; Hwang H-J; Kang J-W; Lee S-J; Chung P-S Enhanced Apoptotic Effect of Combined Modality of 9-Hydroxypheophorbide Alpha-Mediated Photodynamic Therapy and Carboplatin on AMC-HN-3 Human Head and Neck Cancer Cells. *Oncol. Rep* 2009, 21 (2), 329–334. [PubMed: 19148503]
- (50). Rizvi I; Celli JP; Evans CL; Abu-Yousif AO; Muzikansky A; Pogue BW; Finkelstein D; Hasan T Synergistic Enhancement of Carboplatin Efficacy with Photodynamic Therapy in a Three-Dimensional Model for Micrometastatic Ovarian Cancer. *Cancer Res* 2010, 70 (22), 9319–9328. [PubMed: 21062986]
- (51). Kirveliėne V; Grazelele G; Dabkeviėne D; Micke I; Kirvelis D; Juodka B; Didziapetriėne J Schedule-Dependent Interaction between Doxorubicin and mTHPC-Mediated Photodynamic Therapy in Murine Hepatoma in Vitro and in Vivo. *Cancer Chemother. Pharmacol* 2006, 57 (1), 65–72. [PubMed: 16001168]
- (52). He C; Liu D; Lin W Self-Assembled Core–Shell Nanoparticles for Combined Chemotherapy and Photodynamic Therapy of Resistant Head and Neck Cancers. *ACS Nano* 2015, 9 (1), 991–1003. [PubMed: 25559017]
- (53). He C; Agharkar P; Chen B Intravital Microscopic Analysis of Vascular Perfusion and Macromolecule Extravasation after Photodynamic Vascular Targeting Therapy. *Pharm. Res* 2008, 25 (8), 1873–1880. [PubMed: 18446275]
- (54). Rupcich N; Chiuman W; Nutiu R; Mei S; Flora KK; Li Y; Brennan JD Quenching of Fluorophore-Labeled DNA Oligonucleotides by Divalent Metal Ions: Implications for Selection, Design, and Applications of Signaling Aptamers and Signaling Deoxyribozymes. *J. Am. Chem. Soc* 2006, 128 (3), 780–790. [PubMed: 16417367]
- (55). Weng Y-Q; Yue F; Zhong Y-R; Ye B-H A Copper(II) Ion-Selective On–Off-Type Fluoroionophore Based on Zinc Porphyrin–Dipyridylamino. *Inorg. Chem* 2007, 46 (19), 7749–7755. [PubMed: 17705364]
- (56). Lovell JF; Chen J; Jarvi MT; Cao W-G; Allen AD; Liu Y; Tidwell TT; Wilson BC; Zheng G FRET Quenching of Photosensitizer Singlet Oxygen Generation. *J. Phys. Chem. B* 2009, 113 (10), 3203–3211. [PubMed: 19708269]
- (57). Georgakoudi I; Nichols MG; Foster TH The Mechanism of Photofrin Photobleaching and Its Consequences for Photodynamic Dosimetry. *Photochem. Photobiol* 1997, 65 (1), 135–144. [PubMed: 9066293]
- (58). Bonnett R; Martınez, G. Photobleaching of Sensitisers Used in Photodynamic Therapy. *Tetrahedron* 2001, 57 (47), 9513–9547.
- (59). Lovell JF; Jin CS; Huynh E; Jin H; Kim C; Rubinstein JL; Chan WCW; Cao W; Wang LV; Zheng G Porphyrin Nanovesicles Generated by Porphyrin Bilayers for Use as Multimodal Biophotonic Contrast Agents. *Nat. Mater* 2011, 10 (4), 324–332. [PubMed: 21423187]
- (60). Law SL; Chang P; Lin CH Characteristics of Mitoxantrone Loading on Liposomes. *Int. J. Pharm* 1991, 70 (1–2), 1–7.
- (61). Henderson BW; Busch TM; Vaughan LA; Frawley NP; Babich D; Sosa TA; Zollo JD; Dee AS; Cooper MT; Bellnier DA; Greco WR; Oseroff AR Photofrin Photodynamic Therapy Can Significantly Deplete or Preserve Oxygenation in Human Basal Cell Carcinomas during Treatment, Depending on Fluence Rate. *Cancer Res* 2000, 60 (3), 525–529. [PubMed: 10676629]

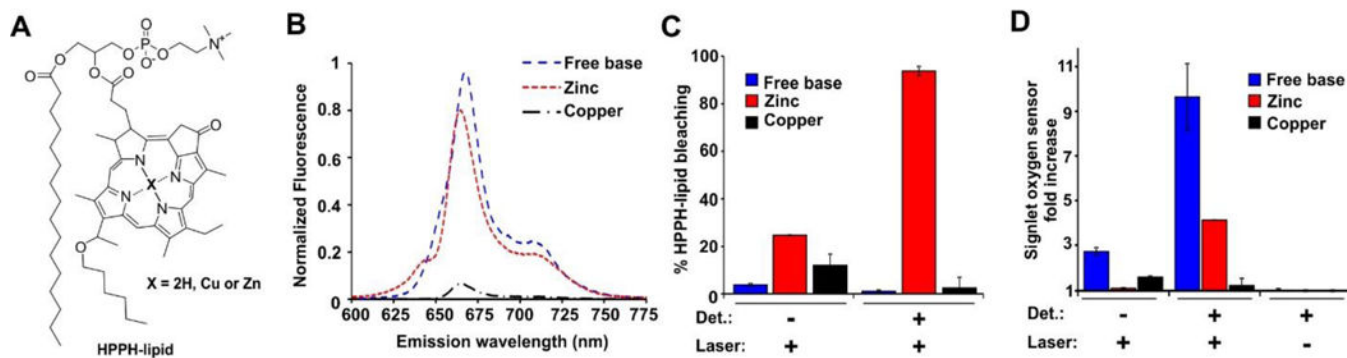


Figure 1: Effect of metal chelation on HPPH-lipid photophysical properties in intact and lysed PoP liposomes.

A) Chemical structure of the HPPH-lipids examined. **B)** Fluorescence emission spectra of an equal concentration of indicated PoP liposomes in phosphate buffered saline. Liposomes were made with [DSPC:Cholesterol:DSPE-PEG2000:HPPH-lipid] at a molar ratio of [50:35:5:10] **C)** Fluorescence bleaching of liposomes following irradiation with 200 mW/cm² of 665 nm laser light for 60 seconds. Triton X-100 detergent (“Det.”) was added to lyse the liposomes. **D)** Singlet oxygen generation was assessed indirectly by examining the increase in fluorescence of singlet oxygen sensor green before and after laser irradiation.

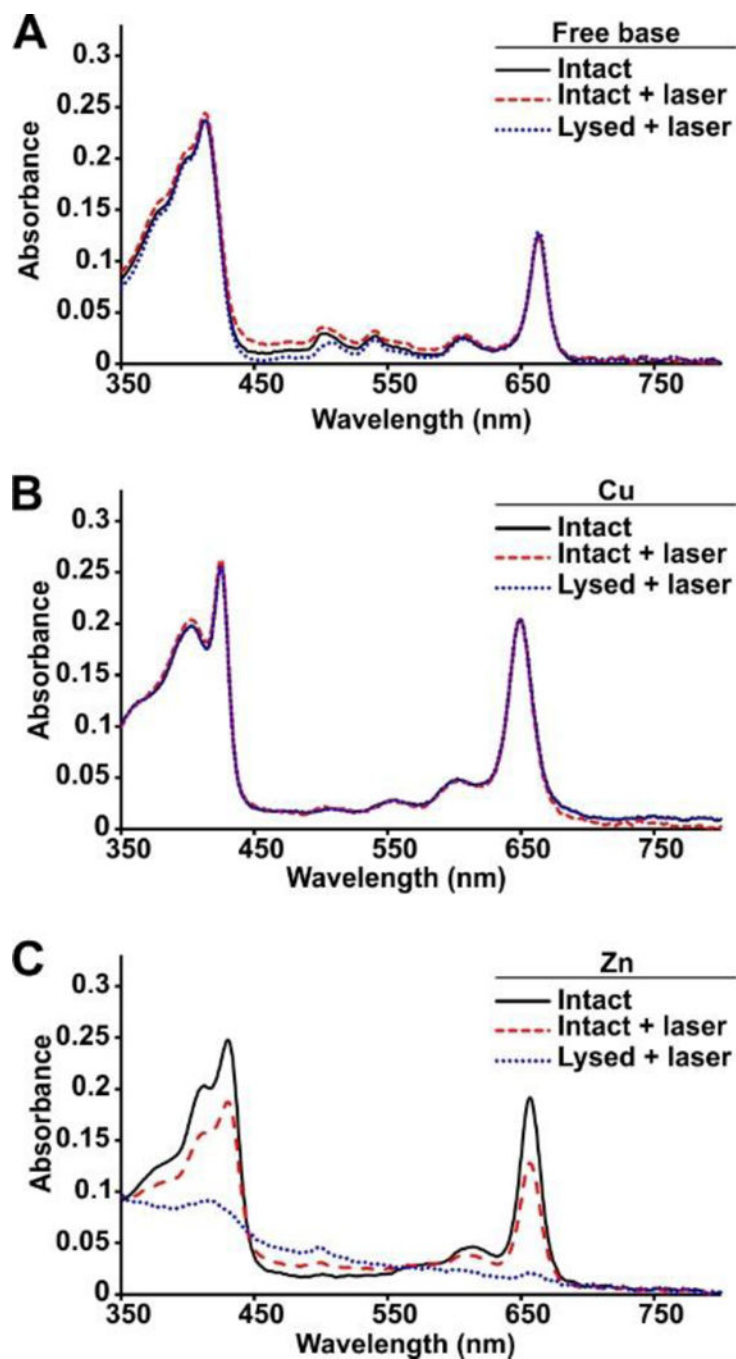


Figure 2: Absorbance spectra of laser-treated PoP liposomes.

Spectra of **A)** Free base, **B)** Cu, and **C)** Zn HPPH-lipid containing liposomes. Spectra were recorded of liposomes which were either untreated, phototreated in liposomal form, or phototreated after being lysed with a 665 nm laser at a fluence rate of 200 mW/cm² for 60 seconds. The respective Soret and Q-band peaks for the intact liposomes were: Free base: 413 and 663 nm; Cu: 425 and 650 nm; Zn: 430 and 657 nm.

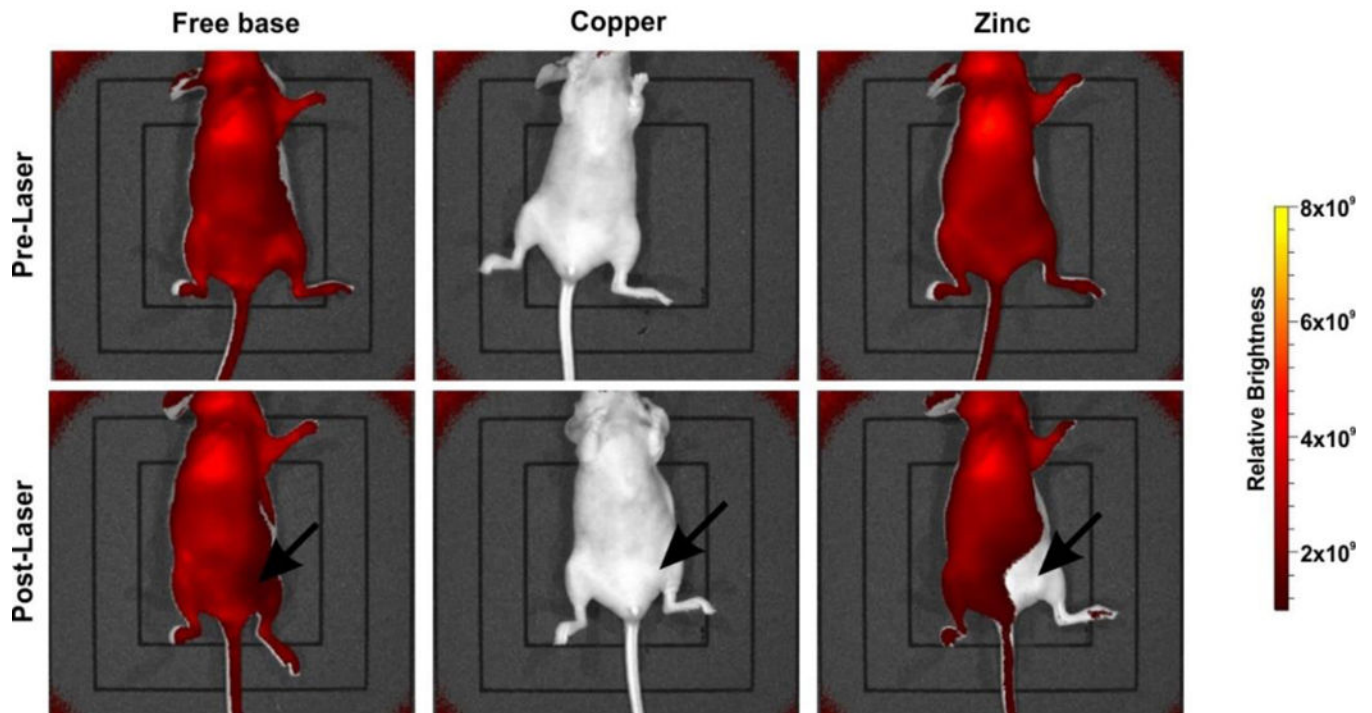


Figure 3: In vivo imaging of HPPH-lipid fluorescence pre- and post- laser exposure. Mice were injected with equivalent doses (11 mg/kg) of free base, Cu and Zn forms of HPPH-lipid. 24 hours post injection mice were imaged and treated with a 665 nm laser at a fluence rate of 200 mW/cm² for 12.5 minutes (150 J/cm²).

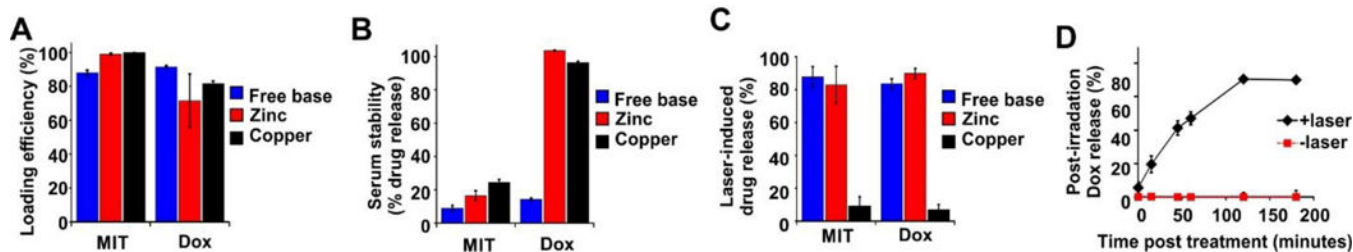


Figure 4: Drug loading and release.

Liposomes containing 10% free base, Cu, and Zn HPPH-lipid were loaded with Dox or MIT.

A) Loading efficiency as assessed with gel filtration to separate free drug from liposomal drug. **B)** Stability in 50% serum after 24 hours and **C)** Light-triggered release of drugs was tested using a G-75 column for MIT and fluorescence quenching for Dox following a 10 minute laser treatment at 200 mW/cm². **D)** Dox release from Cu-PoP liposomes following light treatment.

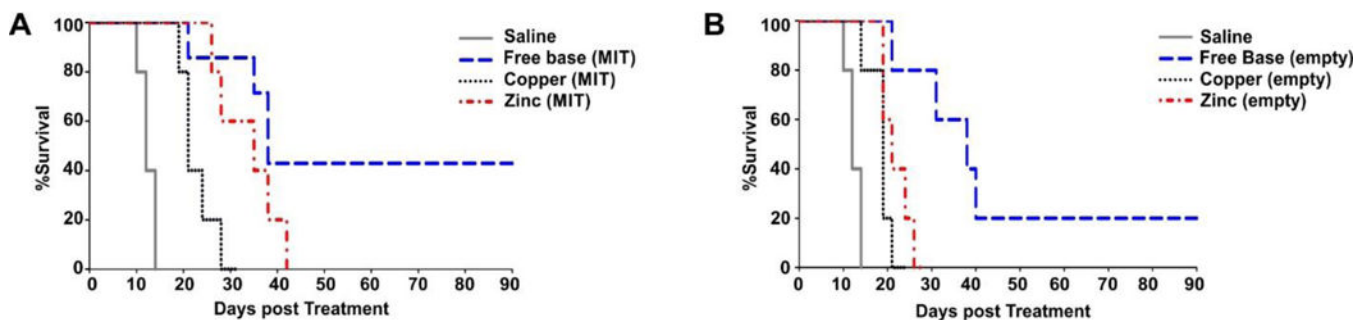


Figure 5: Kaplan-Meier survival curves for nude mice bearing MIA PaCa-2 tumors phototreated immediately post injection.

Mice were IV injected with **A**) 5 mg/kg mitoxantrone liposomes comprising of 10% free base, Cu, and Zn HPPH-lipid, or **B**) equivalent doses of empty liposomes. Mice were treated 10 minutes post injection with a 665 nm laser at 200 mW/cm² for 12.5 minutes (150 J/cm²). Mice were given a single injection and phototreatment and sacrificed when the tumor size was greater than 5 times the initial volume. Based on the log-rank test there was a statistically significant difference between all treatment groups and the saline control ($P < 0.05$). There were no statistically significant differences between the empty and mitoxantrone loaded free base liposomes. There were statistically significant differences between the empty and loaded Cu and Zn HPPH-lipid liposomes ($P < 0.05$)

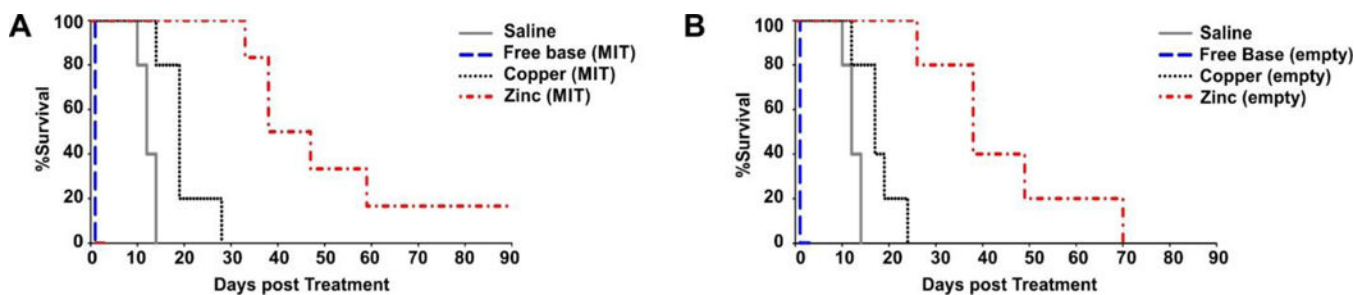


Figure 6: Kaplan-Meier survival curves for nude mice bearing MIA PaCa-2 tumors phototreated 24 hours post injection.

Mice were IV injected with **A**) 5 mg/kg mitoxantrone in 10% free base, Cu, or Zn HPPH-lipid liposomes, or **B**) equivalent doses of empty liposomes. Mice were treated at 24 hours post injection with a 665 nm laser at 200 mW/cm² for 12.5 minutes (150 J/cm²). Mice were given a single injection and laser treatment and were sacrificed when the tumor size was greater than 5 times the initial volume. Mice treated with the free base were all sacrificed within 24 hours of the treatment due to a reduction in body temperature or severe lethargy. Based on the log-rank test there was a statistically significant difference between both Cu and Zn groups and the saline control ($P < 0.05$). However there was no significant differences between the mitoxantrone loaded and empty liposomes.